

R. Heinemann · S. Hinduja · G. Barrow

Use of process signals for tool wear progression sensing in drilling small deep holes

Received: 31 March 2005 / Accepted: 27 September 2005 / Published online: 14 April 2006
© Springer-Verlag London Limited 2006

Abstract Detailed knowledge about the relation between wear progression of a cutting tool and the cutting forces generated is of paramount importance for the development of a tool condition monitoring strategy. This paper discusses the changes in the different process signals with progressing tool wear of small diameter twist drills ($D=1.5$ mm), when drilling boreholes having a depth of 10 times the diameter in plain carbon steel using MQL. The effect of different wear patterns on the process signals is presented. Furthermore, several features, which evolve over the life of the drills, are identified and extracted from the process signals. Knowledge about the evolution of these features can support the user to determine the final tool life stage, so that the drill can be replaced before the final fracture occurs.

Keywords Drilling · End-of-tool-life · Monitoring · Wear

1 Introduction

In the last few years, a growing number of machining processes have been carried out on automatically operating machining centres, checked by an operator only irregularly. In order to reduce the risks of tool breakages, the tools are usually exchanged at fixed intervals, based on tool life assumptions. In drilling, the success of this strategy appears to be questionable, because of large variations in the tool life of identical twist drills [1, 2]. In order to exploit drills optimally, there is an increasing interest in developing systems that constantly monitor the condition of the

tool and initialise a tool change when necessary, rather than relying on fixed tool change intervals.

Most of the monitoring systems designed for industrial use so far try to recognise the incident of a tool fracture, i.e. by capturing an abnormally high cutting force during or after the drill breakage. Others check the condition of the drill every time before it is put into operation, e.g. by moving the drill through a laser beam in order to determine whether the drill is still intact from a macroscopic point of view [3–6]. However, both methodologies have in common that they require the final tool fracture as the trigger for further action, i.e. the replacement of the already broken tool. The incident of a tool fracture however might already have brought about serious damage to the work-piece as well as the machine tool itself. Hence, it is of paramount interest to avoid such tool failure. Therefore, a methodology is required that is capable of recognising a state of severe tool wear prior to the drill's break down, in other words right before the final tool fracture actually occurs.

Nowadays, monitoring the torque and thrust force is the most commonly used method to obtain information about the amount of tool wear in drilling [7]. Besides these cutting forces, the analysis of acoustic emission (AE) has become very popular. Although these signals become much stronger as a drill approaches the end of its life, publications about which cutting force provides the most reliable information about its failure are contradictory [7–10]. O'Donnell et al. [11] noticed a large fluctuation in the signals even between consecutive drilling cycles, which they attributed to chip formation and disposal effects. Kavaratzis [12] also observed fluctuations in the process signals, which made him conclude that deep-hole drilling is a stochastic process, where aspects such as chip evacuation or the state of lubrication have a significant effect on the process signals, and make it rather difficult to establish any kind of tool wear monitoring system. Moreover, it has to be mentioned that most of the research work conducted so far concentrated on drills with a diameter larger than 3 to 5 mm drilling holes of less than 6 times the diameter. Twist drills in the diameter range of 1 to 2 mm were considered only

R. Heinemann (✉) · S. Hinduja · G. Barrow
School of Mechanical, Aerospace and Civil Engineering,
Faculty of Engineering and Physical Sciences,
The University of Manchester,
Sackville Street,
P.O. Box 88 Manchester, M60 1QD, United Kingdom
e-mail: robert.heinemann@manchester.ac.uk
Tel.: +44-0161-3063809
Fax: +44-0161-3063803

peripherally, drilling such small holes with a depth-to-diameter ratio exceeding 5 to 6 even has been entirely neglected.

Due to this lack of knowledge, the objective of this paper is to present, in how far the process signals in deep-hole drilling ($L/D=10$) are affected by the tool wear behaviour of small diameter twist drills ($D=1.5$ mm). Furthermore, several features, some of which are new, are extracted from the process signals and their analysis provides information about the wear progression of the tool and its imminent failure.

2 Experimental setup

Drilling tests were conducted on a CNC milling machine of the portal-frame type. The workpiece material, plain carbon steel with 0.45% carbon (Mat.-No.: 1.0503), was cut into plates of $75 \times 75 \times 15$ mm³ and fixed in a vice mounted on top of a Kistler 2-component dynamometer (9271A), which measured the torque and thrust force, see Fig. 1. Both signals were low-pass filtered (30 Hz cut-off frequency) and passed on to a PC. The AE-signal was detected by a Kistler AE-sensor (8152A1) mounted on top of the machine tool table next to the dynamometer. A schematic diagram of the experimental setup is shown in Fig. 2.

It was observed that the distance of the drilled hole from the centre of the dynamometer had an effect on the torque measured because the eccentric thrust force, coupled with its lever arm, caused a slight misalignment of the platform. Hence, in order to minimise the error in the measured torque values, a row of 7 holes was drilled in the workpiece, with the fourth hole being centred on the dynamometer. Next, 18 boreholes were drilled in a second workpiece but no measurements were recorded for these boreholes. Whilst these holes were being drilled, the first workpiece was manually moved by 2.5 mm so that the next row of 7 holes was also centrally above the dynamometer.

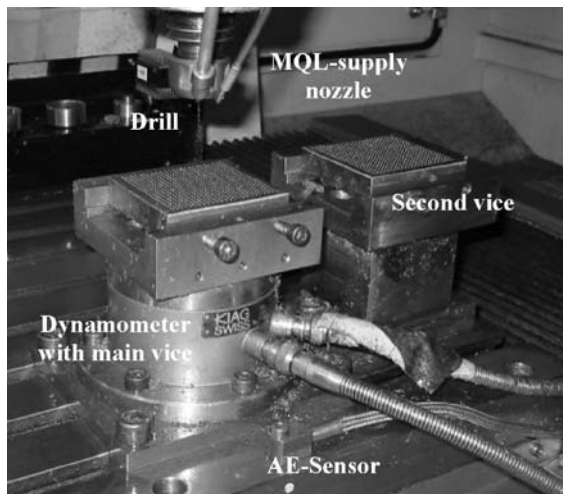


Fig. 1 Test setup for drilling tests

For the drilling tests, a fatty ester minimum quantity lubricant was used, supplied externally via a nozzle attached to the machine's head next to the spindle. An amount of 18 ml/h was supplied.

The tools used were HSS and Co-HSS twist drills, 1.5 mm in diameter. These drills had enlarged chip flutes, a parallel web and a high helix angle, in order to improve chip evacuation in deep-hole drilling [13]. Uncoated drills as well as hardlayer- (TiN, TiCN, TiAlN) and softlayer- (MoS₂) coated drills were tested. For all the drills, a cutting speed of 26 m/min and a feed rate of 0.026 mm/rev were used. This set of cutting parameter was within a tolerance of $\pm 15\%$ of the cutting parameters recommended by the tool manufacturers. In order to avoid tool run-out while drilling the 15 mm deep through-holes into the workpieces, all holes were pre-centred by a pilot hole, which had a diameter of 1.55 mm and depth of 3 mm, as recommended by the manufacturer of the pilot drill, Mikron Tool SA.

The average tool life for each of the 7 drill types tested is shown in Table 1. In the case of the TiN- and TiAlN-coated Co-HSS drills from Titex, the manufacturer provided tool life estimates for the drills employed, which are included in Table 1 as well. It can be seen that the average tool life achieved in the experiments was very similar to the manufacturer's tool life expectation. Because of this close match, it can be assumed that the cutting tests were conducted under cutting conditions comparable to those in industry.

3 Tool wear patterns effecting process signals

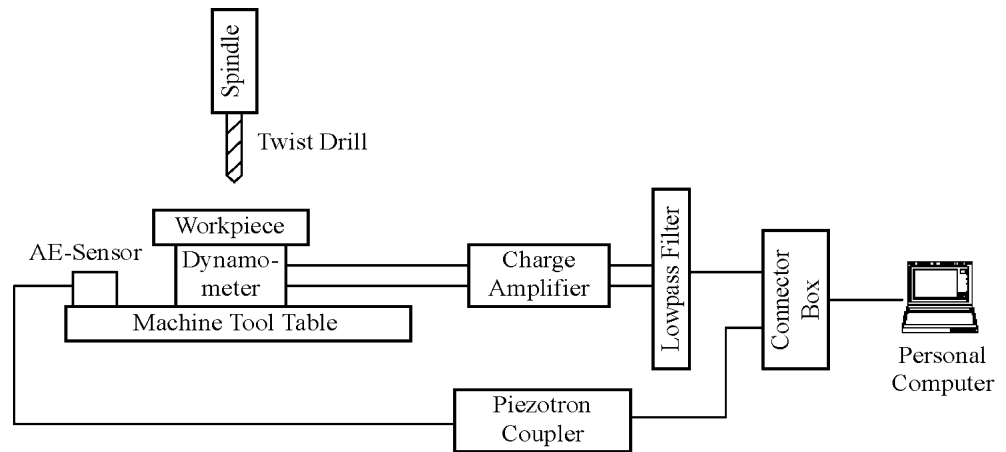
As an example, Fig. 3 shows three-dimensional plots of thrust force, torque and AE-RMS signals obtained with a TiAlN-coated Co-HSS drill, which was able to drill 754 boreholes (denoted as 100%) before fracture occurred. Each drilling cycle was of 6 s duration, using a cutting speed of 26 m/min at a feed rate 0.026 mm/rev. Each borehole was pre-centred by a pilothole 1.55 mm in diameter and a depth of 3 mm.

3.1 Thrust force

As can be seen in Fig. 3a, the thrust force does not show any significant change throughout the entire tool life, resulting in a plateau-like shape. Two peaks occurred at the very end of the tool life, the second and bigger peak during the cycle in which the tool fractured. Such peaks did not always occur; in fact, they were observed for only a very small number of the drills tested. Therefore, these peaks cannot be used as indicators of an imminent tool failure.

In a few rare cases, the thrust force increased slightly from one cycle to another, so that at the end of the tool life, the thrust force was 20 to 30% higher than at the start.

Fig. 2 Schematic diagram of experimental setup



3.2 Torque

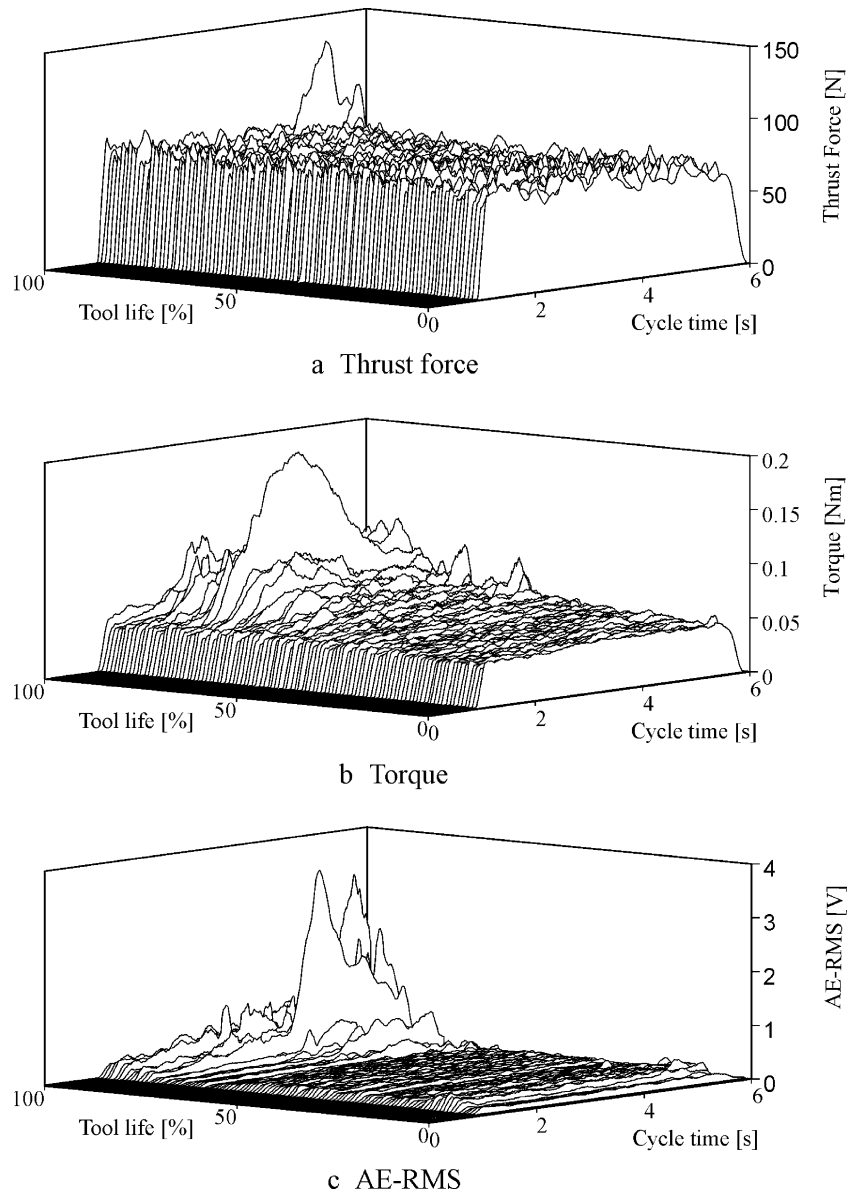
Unlike the thrust force, the torque revealed a much more significant variation during the tool life, as can be seen in Fig. 3b. With progressing tool life, three main changes in the torque signal were observed, which are depicted in more detail in Fig. 4. Firstly, a notable increase in the magnitude during initial penetration, see Fig. 4a, which can be attributed to progressing flank wear and rounding of the cutting edge corners, identified as the typical wear patterns in this operation. Secondly, a growing fluctuation in the signal, caused most likely by a deteriorated chip evacuation and progressing flank and corner wear [14], see Fig. 4a. Thirdly, a change in the general slope of the torque signal, characterised by a shift of that depth at which the torque starts to rise and a significantly higher maximum peak, see Fig. 4b. During the initial period of tool life, a rise in torque was mostly observed at increased borehole depths, usually provoked by serious chip jamming, as can be recognised whilst drilling the 403rd borehole. However, with progressing tool life, the torque started to rise at more moderate borehole depths. These observations, however, were made only for some of the cycles in the latter half of the drill's tool life, as it is shown in Fig. 4c. Therefore, the increase in torque at low borehole depths cannot be solely attributed to the extent of tool wear.

Observations revealed that this change in slope of the torque curve usually occurred during the presence of microwelding of the workpiece material to the drill tip. A plausible explanation for this phenomenon is that the microwelding increased the tool's dullness in addition to the already excessive wear and consequently the drill generated more cutting heat, which, in turn, promoted the evaporation of the minimum quantity lubricant. It is even plausible that the bluntness of the drill caused the breakdown of the lubricant film at the cutting point, associated with strongly increased friction between drill and workpiece. Because of this, the drill generated a torque that abruptly increased after it had been drilling only a few millimetres. The removal of the microwelding led to a reduction in the dullness of the cutting edges and a drop in the torque. The microwelding that was adhered to the tip of the TiAlN-coated drill whilst drilling the 653rd borehole was removed during the initial engagement of the tool during the subsequent, 654th borehole, see Fig. 4c. The removal was most probably triggered by shearing forces exceeding the adhesion forces between the microwelding and the drill. The drill had to suffer from strong microwelding again whilst drilling the 701st borehole, bringing about a strong increase in torque at a very moderate borehole depth, as Fig. 4c reveals. This periodical growth and removal of microwelding was observed several times for the drills employed in this research.

Table 1 Tool life of twist drills tested in the experiments; the number in brackets gives the tool life estimate by the manufacturer (for those drills available)

Drill type	Manufacturer	Drill code	Average tool life [number of holes]
HSS uncoated	Titex	A1222	558
Co-HSS uncoated	Titex	A1249	536
Co-HSS+TiN	Titex	A1249-TiN	709 (653)
Co-HSS+TiAlN	Titex	A1249-TFL	966 (933)
Co-HSS+TiCN	Gühring	GT100-TiCN	604
Co-HSS+TiAlN	Gühring	GT100-Fire	761
Co-HSS+MoS ₂	Gühring	GT100-Molyglide	600

Fig. 3 Development of different process signals over the tool life of a TiAlN-coated Co-HSS drill



3.3 Acoustic emission

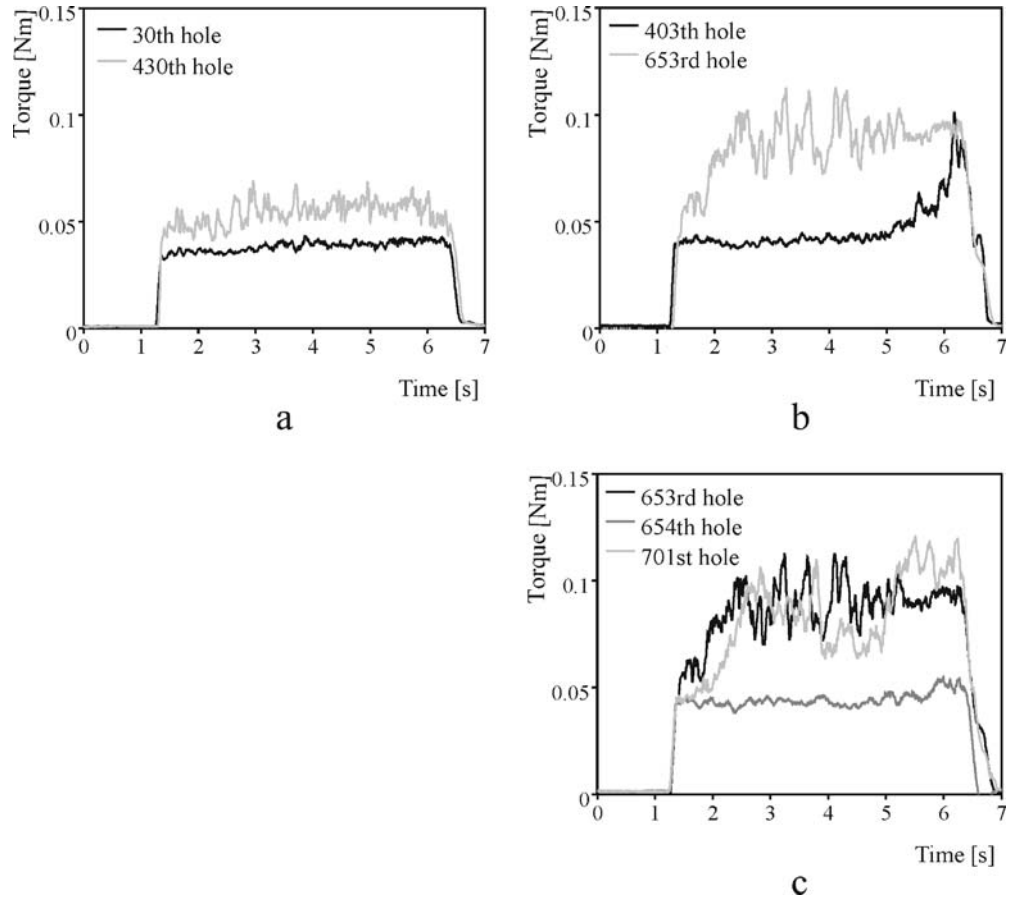
Like the torque, the AE-signal revealed a strong variation during the tool life of the assessed twist drills, see Fig. 3c. In the first two-thirds of their tool life, most drills generated a very low AE-signal. In the last third of their tool life, the AE-signals exhibited two characteristics. Firstly, the maximum AE during each drilling cycle usually occurred at increased depths, probably caused by the chips jamming inside the drill's flutes [15]. Secondly, with growing flank and corner wear, there was an appreciable increase in the overall magnitude of the AE-signal probably caused by an increase in tool vibrations, which can be detected from dynamic components of the cutting forces and AE signals [2]. The rapid rise at greater borehole depths was most likely provoked by the increased dullness of the drill, causing an accelerated evaporation of the minimum quantity lubricant. Hence, the rapidly deteriorating lubrica-

tion condition at the cutting point and inside the drill's flutes caused an increasingly obstructed chip disposal, since the chips had to be evacuated through less-well lubricated flutes.

4 Evolution of process signal features over the tool life

As a result of the observations discussed above, three features were extracted from the process signals. The first two of these were the maximum torque occurring within each drilling cycle and the integral of the AE-RMS signal of each drilling cycle. In contrast to these features, which can be represented by a single numeric value, the description of the torque curve required a more complex analysis. In order to characterise the curve, each drilling cycle was divided into three sections. The first section ranged from a depth of 3 to 6 mm, i.e. it covered the first

Fig. 4 Change in torque generated by a TiAlN-coated drill at different tool life stages



quarter of the drilling process, the second from 6 to 12 mm (second and third quarter), and the last from 12 to 15 mm (final quarter). The integral of each of these sections was calculated, and, finally, the three integrals were compared to each other, see Table 2.

The reason for sectioning the torque curve into three integrals of the aforementioned length is based on the following hypothesis. With a sharp drill (case A), it can be assumed that the second integral is of similar size as the sum of integrals I and III. This will result in a ratio of

approximately one. Tool wear and serious chip jamming, which mostly affected the torque at elevated borehole depths (case B), cause integral III to increase in magnitude, whereas integrals I and II are only slightly affected. Therefore, the sum of integrals I and III is likely to become greater than integral II, and the ratio drops below one. The existence of microwelding, which was observed in association with heavy tool wear and which usually occurred during the final stages of the tool life, moved the point at which the torque begins to rise to lower borehole depths.

Table 2 Sectioning of the torque curve and the relation between the three integrals

Case	Illustration	Relation between sections	Process characteristics
A		$I + III \approx II$	new drill, no chip clogging,
B		$I + III > II$	moderate tool wear, (moderate) chip clogging,
C		$I + III < II$	strong microwelding caused by extensive tool wear, serious chip clogging,

This causes integral II to increase substantially (case C) and the ratio to rise above one.

Figure 5 shows the aforementioned signal features plotted against the overall tool life of three different twist drills. Two curves are shown for TiAlN-coated drills because two such drills were obtained, and tested, from different manufacturers. It can be seen from Fig. 5a that most drills generated the strongest AE-signal during their final tool life stage, i.e. between 80 and 100% tool life. The uncoated HSS drill in contrast generated the strongest AE-signal at 60% tool life, after which the AE-signal decreased again. However, this behaviour can be considered as an exception, since only a very few drills showed such a development in the AE-integral.

For all the drills tested, the maximum torque occurred during the final stages of the tool life, see Fig. 5b. However,

the curve plotted for the uncoated drill is different from the two curves plotted for the TiAlN-coated drills. In the case of the former drill, the maximum torque curve shows an almost steady increase throughout the drill's tool life. For the latter drills, the curves do not exhibit any such increase until about 60% of the tool life, after which the maximum torque increases notably.

By analysing such graphs for all the drills tested, it became apparent that they can be categorised into two groups, based on how the maximum torque within each cycle evolved over the tool life of the drill. The drills in the first group exhibited a comparatively short period in which the maximum torque remained constant; for the rest of the tool life, the maximum torque increased at a steady rate, see Fig. 6a. This group includes all uncoated and MoS₂-coated drills. Various tool life tests conducted have confirmed the

Fig. 5 Development of three features extracted from the process signals in relation to tool life

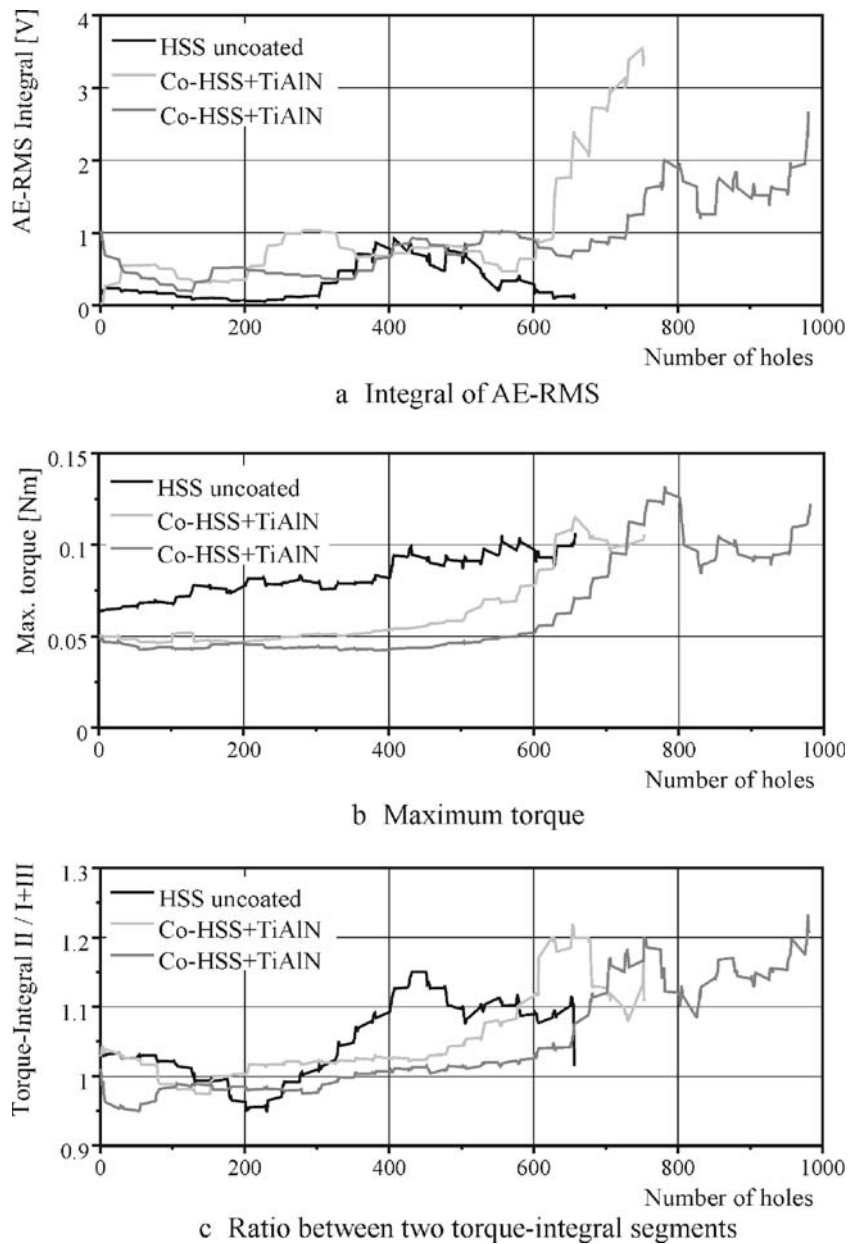
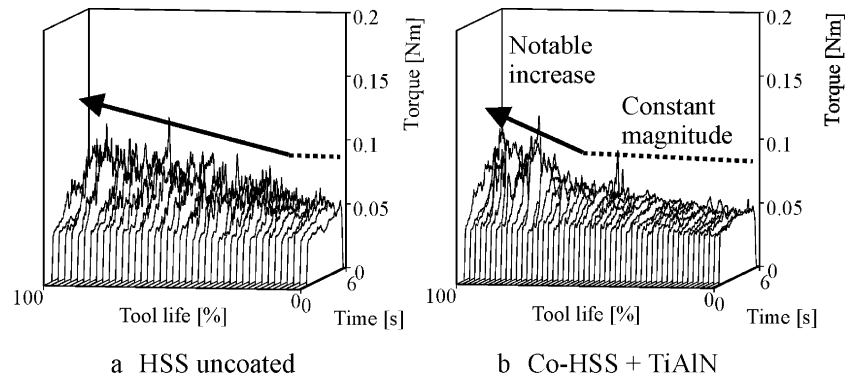


Fig. 6 Evolution of the torque signal of an uncoated and TiAlN (hardlayer) coated twist drill



findings of Toenshoff et al. [16], that MoS_2 -coatings are too soft to bring about a significant reduction in tool wear. Thus, it is not surprising that MoS_2 -coated drills exhibit a wear behaviour similar to that of uncoated drills and show a similar development of the torque signal during their tool life. The second group exhibited a comparatively much longer period during which the maximum torque recorded from each cycle remains constant; for the remaining part of the tool life, as before, the maximum torque increases at a steady rate, see Fig. 6b. This group is represented by the hardlayer-coated drills tested, i.e. TiN, TiCN and TiAlN. It was observed that the coatings' hardness and wear-resistance gave rise to a notable reduction in tool wear and prevented serious material adhesion during a considerable proportion of the overall tool life. However, towards the end of their tool life, when the coating was partially abraded, the coated drills also exhibited serious wear and notable microwelding of workpiece material.

The ratio between the torque integral sections is depicted in Fig. 5c. For new drills, a ratio close to one was calculated, indicating a torque curve with a constant gradient (case A). With progressing tool wear accompanied by serious microwelding, integral II increased markedly, leading to a ratio greater than one (case C). The periodic drop in the torque and the AE signal for one of the TiAlN-coated drills was caused by the shearing of the microwelding. This resulted in a corresponding decrease in the integral-ratio curve.

The superposition of three phenomena, namely, general tool wear progression, presence of microwelding and strong workpiece material adhesion, and the occurrence of chip jamming, occurring to varying extents, led to notable fluctuations in the feature values, as shown in Fig. 5. Although these phenomena are somehow related to each other, for example, extensive tool wear usually promotes microwelding and the presence of microwelding often deteriorates chip disposal, observations suggest a less stringent correlation between them. Serious chip jamming was observed at every stage of the tool life, but it cannot be stated that it occurred more frequently during a particular stage of tool life. Extensive tool wear usually promoted the growth of microwelding which, however, was removed at irregular intervals.

5 Conclusions

A number of conclusions can be drawn from the observations made during the experiments. They provide useful information for the design of a tool wear monitoring methodology for small diameter twist drills in deep-hole drilling:

The thrust force exhibited a very weak correlation with the progression of tool wear and is therefore an inappropriate parameter for monitoring tool wear.

In contrast, the overall level of the torque and AE signal in a cycle tended to increase towards the end of tool life. Hence, these two signals appear to be much more suitable for tool condition monitoring in this particular application than the thrust force.

Strong microwelding of workpiece material, provoked by notable tool wear, caused not only the torque curve to start rising at lower borehole depths but also further increased the maximum torque within a cycle. Usually, the microwelding was removed from the drill after several drilling cycles, causing a less pronounced increase in the torque. The process of growth and removal of microwelding was observed several times for most of the drills employed.

Based on the evolution of the torque over the tool life, the drills tested can be subdivided into two groups, one for hardlayer coated drills and the other for uncoated and softlayer-coated drills.

The extracted features, i.e. maximum torque, integral of AE-RMS and the ratio between two torque-integral sections, exhibited their maximum value during the final stage of tool life for most of the twist drills tested. Unfortunately, they suffered from strong fluctuations, which are probably due to varying extents of tool wear, microwelding and chip clogging. In view of this, an accurate definition of the final tool life stage is rather difficult.

References

1. Soederberg S, Vingsbo O, Nissle M (1982) Performance and failure of high speed steel drills related to wear. *Wear* 75 (1):123–143

2. Koenig W, Kutzner K, Schehl U (1992) Tool monitoring of small drills with acoustic emission. *Int J Mach Tools Manuf* 32 (4):487–493
3. Nordmann K (2001) Kleinste Werkzeugdurchmesser werden sicher ueberwacht. *Maschinenmarkt* 1–2:28–29
4. Nordmann K (2004) Kontrolltechniken sinnvoll kombinieren. *Werkstatt und Betrieb* 9:18–21
5. Nordmann K (2003) Fuehlend statt kuehlend. *Maschine und Werkzeug* 1–2(104):50–51
6. Rehse M (1999) Flexible Ueberwachung bei der Bohr- und Fraesbearbeitung in einer Autonomen Produktionszelle. Dissertation, Technical University Aachen
7. Ertunc HM, Loparo KA, Ocak H (2001) Tool wear condition monitoring in drilling operations using hidden markov models. *Int J Mach Tools Manuf* 41(9):1363–1384
8. Galloway DF (1956) Some experiments on the influence of various factors on drill performance. *Trans ASME* 79(2): 191–231
9. Subramanian C, Strafford KN, Wilks PT, Ward LP, McPhee MA (1993) Performance evaluation of TiN-coated twist drills using force measurement and microscopy. *Surf Coat Technol* 62(1–3):641–648
10. Nagao T, Hatamura Y, Mitsuishi M (1994) In-process prediction and prevention of the breakage of small diameter drills based on theoretical analysis. *Ann CIRP* 43(1):85–88
11. O'Donnell G, Young P, Kelly K, Byrne G (2001) Towards the improvement of tool condition monitoring systems in the manufacturing environment. *J Mat Proc Technol* 119 (1–3):131–139
12. Kavaratzis Y (1990) Deep hole drilling with twist drills – Aspects of the CNC process and its real time monitoring and adaptive control. Dissertation, University of Aston, Birmingham, UK
13. United States Cutting Tool Institute (1989) Metal cutting tool handbook. Industrial Press, New York
14. Weinert K, Adams FJ (1995) Trockenbohren von Stahl mit Cermet, *VDI-Z Spezial Werkzeuge* 137(2):24–26
15. Dong WP, Joe Au YE, Mardapittas A (1994) Characteristics of acoustic emission in drilling. *Tribology* 27(3):169–170
16. Toenshoff HK, Friemuth T, Mohlfeld A, Podolsky C, Urban B (2001) Influence of soft coatings on chip formation and cutting performance. *Proc Materials Week 2001, Munich*, pp 1–8